Research Square

Preprints are preliminary reports that have not undergone peer review.
They should not be considered conclusive, used to inform clinical practice,
or referenced by the media as validated information.

Deicing chemicals and joint distress in concrete highway pavements of southern Kazakhstan: laboratory tests and a field survey

Galiya Assanova
Kazakh Automobile and Road Institute named after LB Goncharov (KazADI)
Assel Nugmanova
a.nugman@yahoo.com
Kazakhstan Road Research Institute (KazDorNII)

Article

Keywords: Deicing salt, Salt scaling, Concrete pavement, Thermal shock, Calcium chloride, Joint deterioration, Kazakhstan

Posted Date: November 9th, 2026

DOI: https://doi.org/10.21203/rs.3.rs-11433020/v1

License: This work is licensed under a Creative Commons Attribution 4.0 International License.
Read Full License

Additional Declarations: No competing interests reported.

Deicing chemicals and joint distress in concrete highway pavements of southern Kazakhstan: laboratory tests and a field survey

Galiya Asanova[1], Assel Nugmanova[2]*

[1] Kazakh Automobile and Road Institute named after L. B. Goncharov (KazADI), Almaty 050061, Kazakhstan. [kazadi.edu.kz]

[2] Kazakhstan Road Research Institute (KazDorNII), 35 Zhekebatyr Street, Astana, Kazakhstan. [qazjolgzi.kz]

* Corresponding author. E-mail: a.nugman@yahoo.com

Highlights

- NaCl on iced concrete cooled the surface by 9 °C in 1 min, inducing up to 3.3 MPa
- $CaCl_2$ and potassium acetate removed about 5% of sample mass in 30 cycles
- A nitrite-phosphate inhibitor cuts $CaCl_2$ mass loss by one third
- Dense silica-fume mortar in 5% NaCl deformed twice as much as sealed prisms
- Clogged joints and 250-700 m expansion-joint spacing explain summer blow-ups

Abstract

Concrete highways built in southern Kazakhstan over the past decade show scaling, spalling and joint failures after a few winters of deicer use. This study combines four data sets to explain that distress. First, temperatures were recorded inside 100 mm concrete cubes held at -5 °C after NaCl was applied to the iced surface: the surface fell to -14 °C within 1 min, and the 8.9 °C difference between the surface and 50 mm depth corresponds to an elastic thermal stress of 2.7-3.3 MPa, close to the direct tensile strength of pavement concrete. Second, concrete specimens were subjected to 30 wetting-drying cycles in water and four deicer solutions. Water and NaCl produced mass gains of 2.2% and 1.5%, whereas $CaCl_2$, $CaCl_2$ with a nitrite-phosphate corrosion inhibitor and potassium acetate produced mass losses of 5.2%, 3.5% and 5.0%. Third, prisms of a dense silica-fume mortar (water/binder ratio 0.24) immersed in 5% NaCl reached a length change of 0.66 mm/m after 300 h, about twice that of sealed or air-cured companions. Fourth, a condition survey of six concrete highways found scaling, through-cracks, spalling and blow-ups; expansion joints were spaced 250-700 m apart against a design value of 50 m, and contraction joints were packed with deicing grit. Thirty joints monitored at km 181 of the Almaty-Shelek-Khorgos highway closed by 0.81 ± 0.94 mm on average, and two of them took

29% of the total closure. The results support restricting calcium-based and acetate deicers on these pavements, resealing joints before each summer, and restoring the designed expansion-joint spacing.

Keywords: Deicing salt; Salt scaling; Concrete pavement; Thermal shock; Calcium chloride; Joint deterioration; Kazakhstan

1. Introduction

Kazakhstan has built several hundred kilometers of jointed plain concrete pavement since the early 2010s, much of it on the Western Europe-Western China transit corridor between Khorgos, Almaty, Taraz and Shymkent. These roads cross a climate that is hard on concrete from both ends of the thermometer. Southern Kazakhstan falls mainly in the cold semi-arid (BSk) and hot-summer continental (Dsa/Dfa) Köppen classes [1]; pavement surfaces reach 60-70 °C in July and air temperatures fall below -25 °C in January. In winter, road operators spread sodium chloride and sand-salt mixtures to keep traffic moving. Within a few seasons, many sections showed surface scaling of the kind shown in Fig. 1.

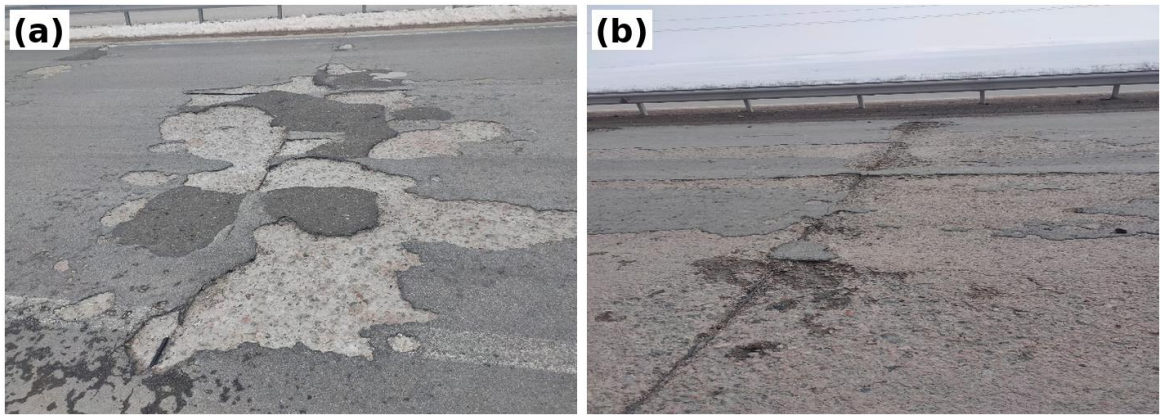


Fig. 1. Deicer scaling on a concrete highway in Kazakhstan: (a) loss of mortar and exposure of coarse aggregate over most of the slab surface; (b) scaling concentrated along a transverse joint.

Salt scaling is the progressive loss of small flakes of mortar from a concrete surface exposed to freezing in the presence of a dilute salt solution. Laboratory work since the 1950s has established its main features: damage peaks at solute concentrations of about 3% by mass and falls at higher concentrations, the effect is largely independent of the solute used, and scaling in salt solution far exceeds scaling in pure water [2,3]. Several mechanisms have been proposed, including hydraulic and osmotic pressure [4], ice-lens growth [5], salt crystallization [6] and the glue-spall mechanism, in which a brine ice layer bonded to the surface cracks on cooling and carries fragments of mortar with it [7-9]. A recent review summarized these physical processes together with the chemical interactions and protective measures reported for concrete pavements [10].

Chemistry matters as much as physics once deicers other than NaCl are used. Calcium chloride reacts with portlandite to form calcium oxychloride, an expansive phase that can form above 0 °C when the $CaCl_2$ concentration in the pore solution is high [11,12]. Chloride binding by aluminate phases produces Friedel's salt, and exposure to concentrated NaCl lowers the flexural

strength of cement paste through crystallization pressure [13]. Acetate and formate deicers, often promoted as chloride-free alternatives, increase portlandite solubility and supply alkalis that can drive alkali-silica reaction [14]. Comparative studies have ranked common deicers by the damage they cause [15-19]; Wang et al. found that $CaCl_2$ solutions were the most damaging of five products tested and that potassium acetate caused only minor scaling [15].

Two gaps motivate the present work. The first is geographical. Almost all published deicer studies come from humid cold regions of North America, northern Europe and China, where pavements rarely exceed 50 °C in summer. In southern Kazakhstan, the annual range of slab temperature approaches 100 °C, so joints that are clogged with deicing grit in winter must accommodate large thermal expansion a few months later. Joint deterioration linked to fluid absorption and deicer phase changes is well documented in the United States [20], and pavement growth after joint closure has been analyzed from long-term joint movement data [21], but we have found no study that links the laboratory behavior of deicers to field distress on concrete highways in Central Asia. The second gap is practical: Kazakh road agencies need evidence to choose between NaCl, $CaCl_2$, inhibited $CaCl_2$ and acetate products, and to decide whether joint maintenance or pavement design is the more urgent problem.

This paper addresses both gaps with four linked data sets: (i) the temperature field and thermal stress in concrete when NaCl is applied to an iced surface; (ii) the mass change of concrete specimens in water and four deicer solutions under wetting-drying cycles; (iii) the deformation of a dense silica-fume mortar immersed in 5% NaCl; and (iv) a condition survey of six concrete highways in southern Kazakhstan, including 30 monitored joints. Section 2 describes the methods, Section 3 the results, and Section 4 interprets them and draws out recommendations for practice.

2. Materials and methods

2.1. Thermal response to NaCl application

Concrete cubes with 100 mm sides were cast from a pavement mix and cured for 28 days. The cubes were then conditioned at -5 °C for 48 h in a climatic chamber so that the whole section reached a uniform temperature. Sodium chloride was applied to the iced top surface, and temperatures were recorded at the surface and at depths of 1, 5, 10 and 50 mm at 0.5, 1, 2, 3, 4, 5 and 6 min after application.

Melting ice draws latent heat from the concrete, so the surface cools faster than the interior. A thin surface layer that contracts relative to a thick, cooler-changing substrate is restrained in two directions, and its tensile stress can be estimated from linear elasticity:

$$\sigma_b = E\,\alpha\,\Delta T / (1 - \nu) \quad (1)$$

where ΔT is the temperature difference between the surface and 50 mm depth (°C), E the elastic modulus, α the coefficient of thermal expansion and ν Poisson's ratio. The uniaxial estimate, $\sigma_u = E\,\alpha\,\Delta T$, is reported as a lower bound. Typical values for pavement concrete were used, E = 30 GPa, $\alpha = 10 \times 10^{-6}\,°C^{-1}$ and $\nu = 0.2$ [22,23], so that $\sigma_u \approx 0.30\Delta T$ MPa. Both estimates ignore creep and are therefore upper bounds on the stress actually carried by the material during the first minutes after application.

2.2. Mass change in deicer solutions

Concrete specimens were exposed to five solutions: distilled water as the reference, sodium chloride (NaCl), calcium chloride ($CaCl_2$), calcium chloride with a nitrite-phosphate corrosion inhibitor ($CaCl_2$ + inhibitor) and potassium acetate (CH_3COOK) Fig. 2a shows the specimens during exposure. Each cycle consisted of wetting followed by drying. Specimens were weighed to 0.1 g every 5 cycles up to 30 cycles, following the weighing procedure of GOST 12730.1 [24]. The mass change after N cycles was calculated as

$$\Delta m_N = (m_N - m_0) / m_0 \times 100\% \quad (2)$$

where m_0 is the mass before the first cycle. The rate of mass change was taken as the slope of a least-squares line through the data from 5 to 30 cycles.

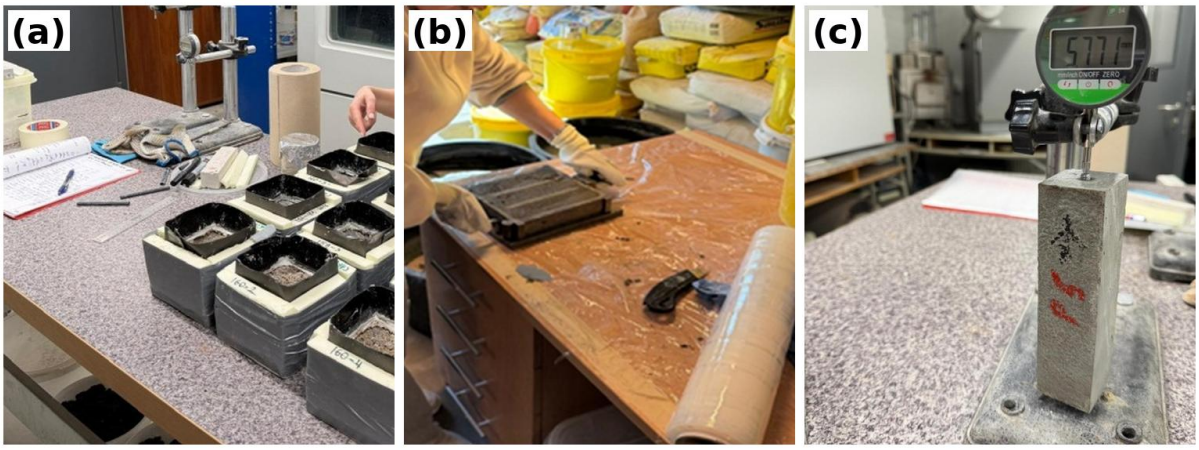


Fig. 2. Laboratory work: (a) concrete specimens exposed to deicer solutions; (b) casting the silica-fume mortar prisms at Riga Technical University; (c) length measurement of a 40 × 40 × 160 mm prism with a digital dial gauge.

2.3. Deformation of dense mortar prisms in NaCl

A dense mortar based on an ultra-high-performance concrete (UHPC) matrix, without fibers, was mixed at the laboratory of Riga Technical University (Table 1). The binder contained 15% silica fume by mass, the water/binder ratio was 0.24 and the sand/binder ratio was 1.10. Dry constituents were mixed until uniform, water containing the dissolved superplasticizer was added, and mixing continued until a homogeneous, highly flowable mortar was obtained. Twelve 40 × 40 × 160 mm prisms were cast (Fig. 2b), with steel studs embedded in the end faces to seat a dial gauge.

Table 1. Composition of the silica-fume mortar. Per-cubic-meter quantities are calculated from the batch masses assuming particle densities of 3150 (cement), 2650 (sand), 2200 (silica fume) and 1070 kg/m ^{3} (superplasticizer).

Constituent	Batch weight (kg)	Per m ^{3} (kg)	Ratio to binder
Portland cement	4.950	835	0.85
Silica fume	0.874	147	0.15
Sand, 0-2 mm	6.406	1081	1.10
Water	1.399	236	0.24
Superplasticizer	0.153	26	0.026

The prisms were demoulded after 24 h and assigned to five storage conditions at 20 ± 2 °C: sealed in plastic film (3 prisms), air-dry (3 prisms), and immersion in NaCl solutions of 5%, 10% and 15% by mass (2 prisms each), prepared from distilled water and technical-grade NaCl. This paper reports the 5% NaCl group together with the sealed and air-dried references; the 10% and 15% groups are still under test. Length was read with a digital dial gauge of 0.01 mm resolution mounted on a rigid stand (Fig. 2c), immediately after demoulding and then at 27, 34, 46, 60, 84, 108, 132, 156, 180, 228 and 300 h. Length change was expressed in mm/m over the 155 mm gauge length, with positive values denoting shortening. Initial prism masses ranged from 580.5 to 599.8 g (mean 591.3 g, standard deviation 7.0 g), which corresponds to a bulk density of about 2310 kg/m ^{3} . Surfaces were inspected under optical magnification for cracking at each reading.

2.4. Field survey and joint monitoring

Visual and instrumental condition surveys were carried out on six concrete-paved highway sections in southern Kazakhstan: Shymkent-Taraz, Shymkent-Saryagash (towards Tashkent), Shymkent-Turkestan, Taraz-Almaty, Almaty-Khorgos and Almaty-Kapshagay. Each distress was photographed, classified and measured: crack and joint widths with a vernier caliper,

lengths with a tape, and vertical displacements with a straightedge and rule. Pavement surface temperatures were measured at selected locations. Cores were taken at selected locations. All work was done under lane closure with warning signs and portable barriers.

To quantify joint movement, tell-tale gauges were fixed across 30 consecutive transverse joints at km 181 of the Almaty-Shelek-Khorgos highway. The joint width and the tell-tale width were recorded at installation and again at removal in June 2025, both with a caliper to 0.1 mm. Assuming a slab length of 5 m, the 30 joints span about 150 m of pavement.

Free thermal elongation of a pavement segment between working expansion joints was estimated as

$$\Delta L = \alpha \, L \, \Delta T \quad (3)$$

where L is the distance between expansion joints and ΔT the change in mean slab temperature, to compare the thermal movement demand with the width of the expansion joints found in the field [26].

3. Results

3.1. Temperature field and thermal stress after NaCl application

Table 2 and Fig. 3a show how fast the surface responded. The surface temperature dropped from -5.0 °C to -12.0 °C in the first 30 s, a cooling rate of about 14 °C/min, and reached a minimum of -14.0 °C after 1 min. Below the surface the response was damped and delayed: at 1 mm the minimum was -9.0 °C at 2 min, at 10 mm -7.2 °C at 3-4 min, and at 50 mm the temperature changed by only 0.6 °C over 6 min. The steepest gradient therefore sat in the outer millimeter, where the temperature difference reached 5.5 °C at 1 min.

Table 2. Concrete temperature after NaCl application to the iced surface of a cube pre-conditioned at -5 °C, and the corresponding thermal stress estimates.

Time (min)	Surface (°C)	1 mm (°C)	5 mm (°C)	10 mm (°C)	50 mm (°C)	ΔT (°C)	σ_u (MPa)	σ_b (MPa)
0	-5.0	-5.2	-5.1	-5.0	-5.0	0.0	0.00	0.00
0.5	-12.0	-7.5	-6.5	-5.5	-5.0	7.0	2.10	2.63
1	-14.0	-8.5	-7.8	-6.2	-5.1	8.9	2.67	3.34
2	-12.5	-9.0	-8.5	-7.0	-5.2	7.3	2.19	2.74
3	-11.0	-8.9	-8.5	-7.2	-5.3	5.7	1.71	2.14
4	-10.0	-8.7	-8.3	-7.2	-5.4	4.6	1.38	1.73
5	-9.2	-8.5	-8.0	-7.1	-5.5	3.7	1.11	1.39
6	-9.0	-8.3	-7.8	-7.0	-5.6	3.4	1.02	1.28

ΔT = difference between 50 mm depth and surface. $\sigma_u = E\alpha\Delta T$; $\sigma_b = E\alpha\Delta T/(1 - \nu)$, with E = 30 GPa, $\alpha = 10 \times 10^{-6}$ °C^{-1}, $\nu = 0.2$.

The largest surface-to-50 mm difference, 8.9 °C at 1 min, gives $\sigma_u = 2.67$ MPa and $\sigma_b = 3.34$ MPa (Fig. 3b). The biaxial value falls within the 3-4 MPa range of direct tensile strength typical of pavement concrete [22]. The biaxial estimate stayed above 2 MPa for about 3 min and decayed to 1.0-1.3 MPa after 6 min as the interior cooled and the surface warmed back towards the brine temperature. These values are larger than the 1.3 MPa for a 4.3 °C drop reported in earlier work reviewed by Zhang et al. [10], mainly because the surface drop measured here was twice as large.

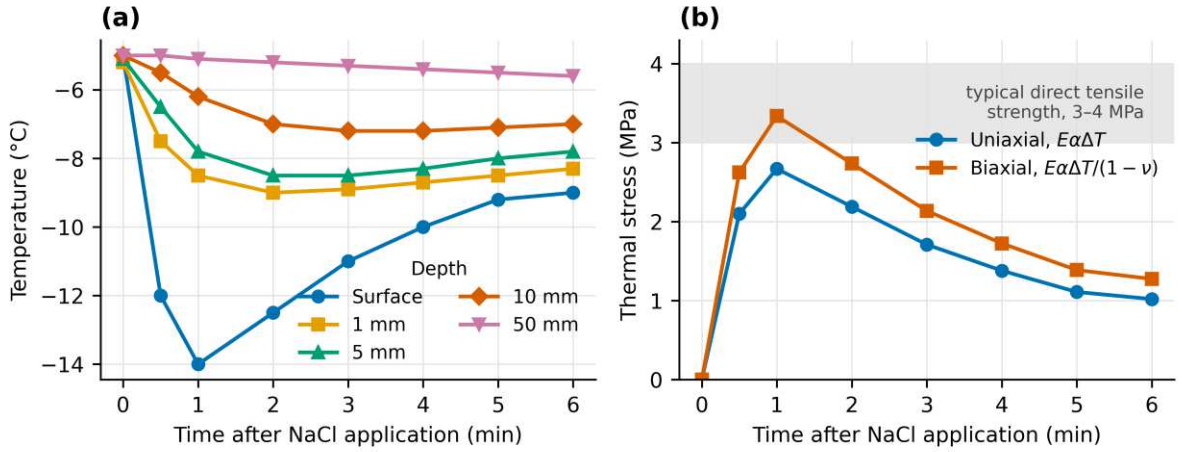


Fig. 3. Response of concrete pre-conditioned at -5 °C to NaCl applied on the iced surface: (a) temperature at the surface and at four depths; (b) uniaxial and biaxial elastic thermal stress from the surface-to-50 mm temperature difference.

3.2. Mass change in water and deicer solutions

The five solutions split into two groups (Table 3, Fig. 4). Specimens in water and NaCl gained mass throughout the 30 cycles, by 2.2% and 1.5%, with gains that slowed down as the pores filled. Specimens in $CaCl_2$, inhibited $CaCl_2$ and potassium acetate lost mass at nearly constant or increasing rates. After 30 cycles the losses were 5.2% for $CaCl_2$, 5.0% for potassium acetate and 3.5% for inhibited $CaCl_2$. The least-squares rates between 5 and 30 cycles were -0.188, -0.170 and -0.130% per cycle for these three solutions, against +0.055 and +0.035% per cycle for water and NaCl.

Table 3. Specimen mass (g) and mass change (%, in brackets) during wetting-drying cycles.

Cycles	Water	NaCl	$CaCl_2$	$CaCl_2$ + inhibitor	Potassium acetate
0	2448.9	2450.9	2457.9	2452.6	2450.8
5	2468.5 (+0.8)	2465.6 (+0.6)	2445.6 (-0.5)	2445.2 (-0.3)	2431.2 (-0.8)
10	2478.0 (+1.2)	2473.0 (+0.9)	2428.5 (-1.2)	2432.9 (-0.8)	2414.0 (-1.5)
15	2485.7 (+1.5)	2477.9 (+1.1)	2408.8 (-2.0)	2420.7 (-1.3)	2394.4 (-2.3)
20	2493.0 (+1.8)	2482.8 (+1.3)	2384.0 (-3.0)	2403.5 (-2.0)	2372.3 (-3.2)
25	2497.9 (+2.0)	2485.4 (+1.4)	2359.6 (-4.0)	2383.9 (-2.8)	2350.3 (-4.1)

Cycles	Water	NaCl	$CaCl_2$	$CaCl_2$ + inhibitor	Potassium acetate
30	2502.8 (+2.2)	2487.7 (+1.5)	2330.0 (-5.2)	2366.7 (-3.5)	2328.0 (-5.0)

Initial masses (cycle 0) are back-calculated from the recorded masses and percentage changes at 10-30 cycles, which agree to within 0.3 g; masses at 5 cycles are calculated from the recorded percentages.

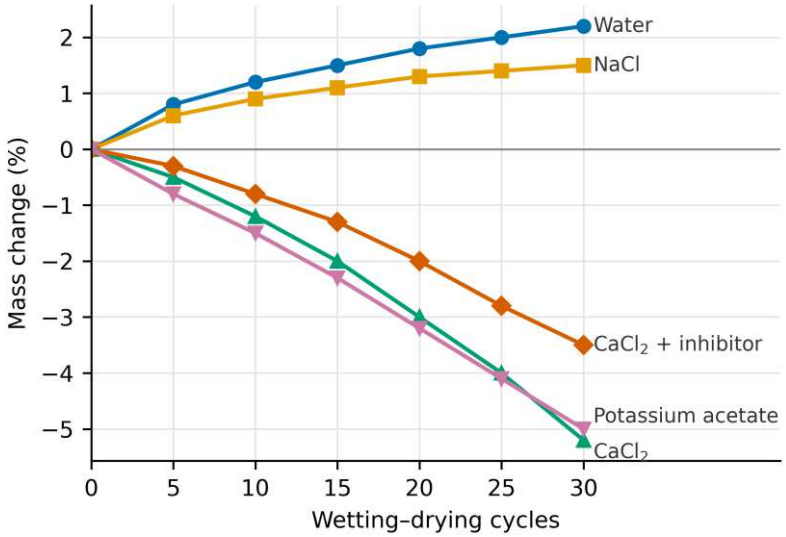


Fig. 4. Mass change of concrete specimens during wetting-drying cycles in water and four deicer solutions.

The time profiles differ within the losing group. Potassium acetate removed the most mass in the first 5 cycles (0.8%) and then continued at a steady 0.7-0.9% per 5 cycles. $CaCl_2$ started more slowly (0.5% in the first 5 cycles) but accelerated, losing 1.2% between cycles 25 and 30, and overtook the acetate after 25 cycles. The inhibitor delayed the loss rather than stopping it: inhibited $CaCl_2$ lost 0.3% in the first 5 cycles and 0.7-0.8% per 5 cycles from cycle 20 onwards, so the gap to plain $CaCl_2$ widened only slowly. At 30 cycles the inhibitor had reduced the total loss by 33%.

3.3. Deformation of silica-fume mortar in 5% NaCl

All three groups of prisms moved in the same direction, but at different rates (Fig. 5). During the first 27 h after demoulding the readings were within ±0.02 mm/m of zero. Between 27 and 84 h, the prisms immersed in 5% NaCl reached 0.35 mm/m, against 0.23 mm/m for the air-dry and 0.12 mm/m for the sealed prisms. After about 130 h the air-dry prisms leveled off at 0.28-0.32 mm/m, while the sealed prisms continued steadily to 0.34 mm/m at 300 h. The immersed prisms kept deforming throughout, adding 0.14 mm/m between 180 and 300 h, and reached 0.66 mm/m at 300 h, 1.9 times the sealed value and 2.1 times the air-dry value.

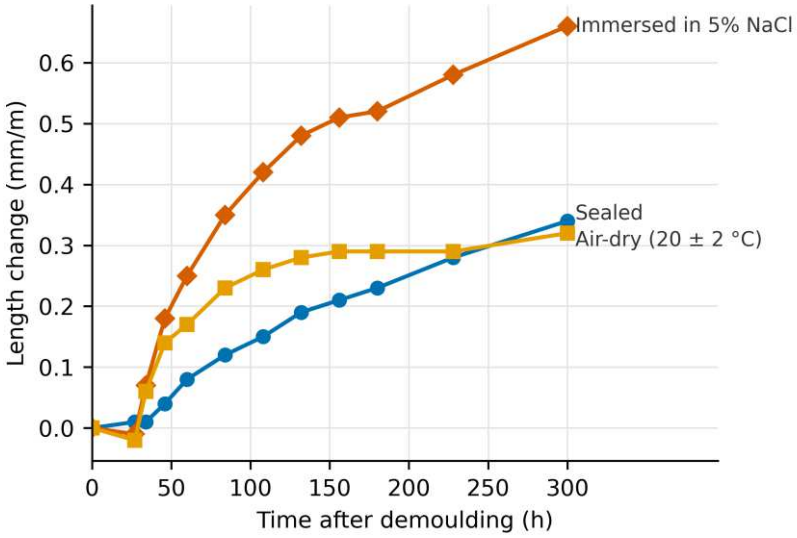


Fig. 5. Length change of 40 × 40 × 160 mm silica-fume mortar prisms stored sealed, in air at 20 ± 2 °C, and immersed in 5% NaCl solution (mean of each group).

3.4. Distress on the surveyed highways

Table 4 lists the distress types found on each section, and Fig. 6 shows representative examples. Three families of distress appeared on every route. Surface scaling ranged from shallow mortar loss to depths of 5 mm (Almaty-Kapshagay) and 10 mm (Almaty-Khorgos), and was worst where water ponded, on acceleration lanes and next to joints. Joint defects included sealant extruded from or missing in the joints, joints packed with sand and deicing grit, spalled joint edges up to 20 mm deep, and horizontal offsets of up to 5 mm. Cracks included longitudinal through-cracks up to 8 mm wide and 15 m long, diagonal through-cracks 5 mm wide crossing several slabs, and transverse cracks from 0.4 mm to 5 mm wide.

Table 4. Distress recorded on the surveyed concrete highways.

Section	Distress	Measured dimensions and observations
Shymkent-Taraz	Slab buckling (blow-up)	Vertical rise 50-70 mm, most visible at slab edges
	Diagonal crack	5 mm wide, through-depth, crossing several slabs; a second crack on the ramp
	Longitudinal cracks	Through-depth; 8 mm wide over 15 m; 2 mm wide over two slabs
	Spalling at joints	Up to 20 mm deep at joint intersections; surface temperature 45 °C
Shymkent-Saryagash	Clogged expansion joint	15 mm joint filled with loose granular material
	Sealant extrusion, scaling	12 mm joint; spalls where sealant was extruded
	Transverse cracks	1 mm wide, attributed to compression
Shymkent-Turkestan	Scaling	Surface temperature 48 °C on concrete and 54 °C on adjacent microsurfacing

Section	Distress	Measured dimensions and observations
Taraz-Almaty	Blow-up at joint	Slabs pushed up and crushed at the joint; 59.5 °C on concrete, 70 °C on asphalt
	Scaling of repair concrete	Expansion joints every 250 m; dowel bars not detected at the joint
	Joint offset	Joints up to 10 mm wide; sealed-over cracks; horizontal offset 5 mm
	Longitudinal and transverse cracks	1 mm wide; joint width 4 mm
Almaty-Khorgos	Scaling and edge breakage	Scaling up to 10 mm deep over the entire acceleration-lane slab; 4 mm joints without sealant; cracks up to 1 mm
Almaty-Kapshagay	Scaling	Up to 5 mm deep where drainage is poor; cracks 0.4 mm; 10 mm joints with sealant extruded or missing and filled with incompressibles
	Spalling	Broken slab edges and corners
	Transverse crack	Through-depth, 5 mm wide, 7 m long

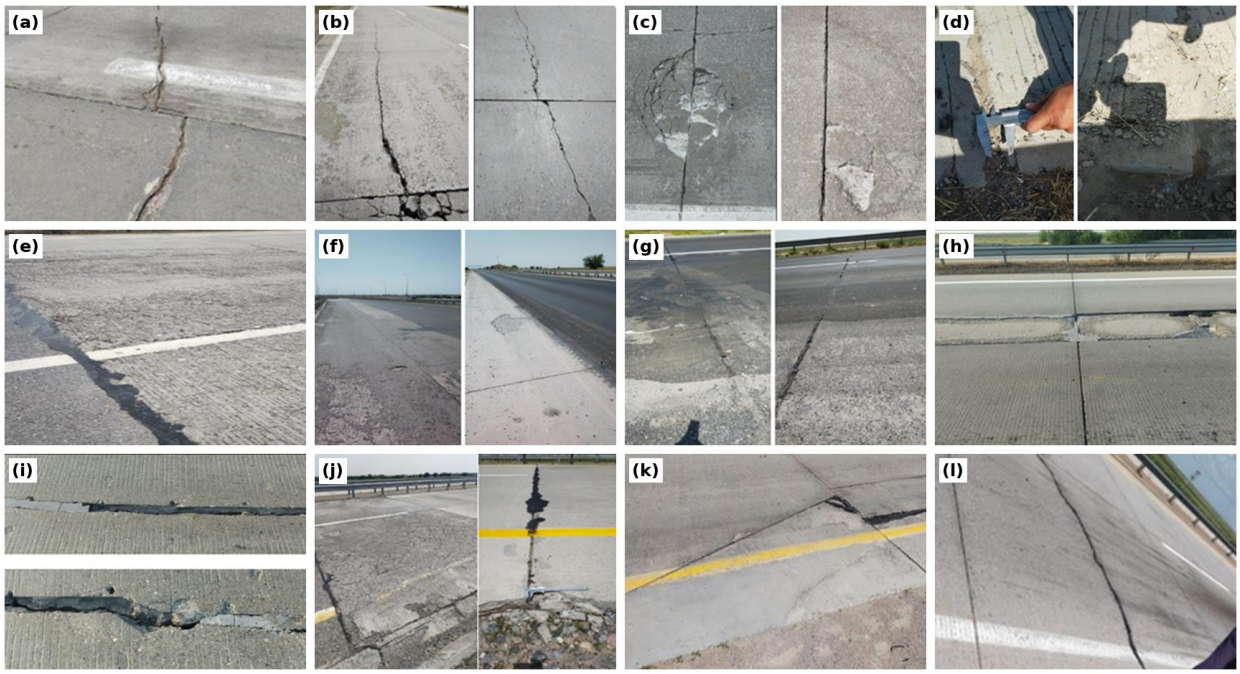


Fig. 6. Representative distress: (a) diagonal through-crack, (b) longitudinal through-cracks and (c) spalling at a joint intersection, Shymkent-Taraz; (d) expansion joint packed with granular material and (e) extruded sealant with surface scaling, Shymkent-Saryagash; (f) scaling and (g) blow-up at a joint, Shymkent-Turkestan; (h) scaling of repair concrete and (i) joint offset, Taraz-Almaty; (j) scaling and joint damage, Almaty-Khorgos; (k) scaling and (l) transverse through-crack, Almaty-Kapshagay.

The joint layout departed from the design. On the sections in the Turkestan region, working expansion joints were found 300-700 m apart, and on Taraz-Almaty every 250 m, whereas the design for Almaty-Khorgos specifies 50 m. The contraction joints had not been maintained and were filled with deicing material at the time of the survey. Blow-ups were recorded on Shymkent-Turkestan, Shymkent-Saryagash and Shymkent-Taraz in the Turkestan region, where the highest pavement temperatures were measured. No blow-ups have been recorded

over the service life of the sections in the Zhambyl region, where mean summer air temperatures are about 5 °C lower.

3.5. Joint movement at km 181

Of the 30 monitored joints, 26 narrowed, 2 did not change and 2 widened between installation and June 2025 (Fig. 7a, Appendix A). The mean change in joint width was -0.81 mm (standard deviation 0.94 mm, median -0.80 mm), and the total closure over the 30 joints was 24.4 mm. Movement was uneven: joints 1 and 10 closed by 4.0 and 3.0 mm and together accounted for 29% of the total, whereas 11 joints moved by 0.5 mm or less. The two joints that widened, by 0.5 and 0.9 mm, were joints 4 and 12. Tell-tale widths increased by 0 to 5.5 mm (total 30.3 mm).

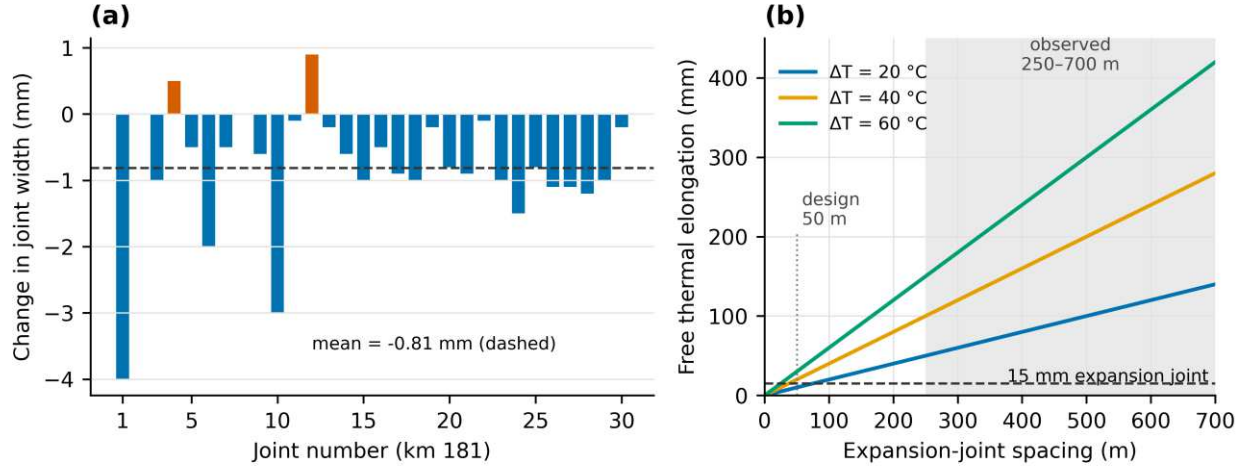


Fig. 7. (a) Change in width of 30 consecutive transverse joints at km 181 of the Almaty-Shelek-Khorgos highway between installation and June 2025 (blue: closure; orange: opening). (b) Free thermal elongation of a pavement segment as a function of expansion-joint spacing for mean slab temperature changes of 20, 40 and 60 °C (Eq. (3), $\alpha = 10 \times 10^{-6}$ °C^{-1}), compared with the design spacing, the spacings found in the survey and a 15 mm expansion joint.

4. Discussion

4.1. Thermal shock as a scaling driver

Laboratory freeze-thaw protocols cool specimens at rates of a few degrees per hour [27,28]. The surface in our test cooled at about 14 °C per minute, two orders of magnitude faster, because melting ice drew heat from the concrete faster than it could be conducted from below. Earlier analyzes of cooling rate concluded that hydraulic pressure and bulk thermal stress in standard tests stay well below the fatigue limit of concrete [10]; those conclusions apply to slow, uniform cooling. The stress we estimate is concentrated in the outer few millimeters, where the temperature difference reached 5.5 °C across 1 mm, and it approaches the tensile

strength at the depth range where scaling flakes originate [3]. The surface mortar layer is also the weakest part of the section, being richer in paste and more porous than the bulk [29].

One application does not scale a sound surface; the estimated peak of 3.3 MPa is an elastic upper bound and lasts less than 2 min. The concern is repetition. In southern Kazakhstan, pavements pass through 0 °C on many winter days, and each deicer application during a cold spell imposes a new thermal shock on a surface already weakened by the previous one. This fatigue-type loading adds to the glue-spall mechanism [7,9] and supports treating the frequency of deicer application, and not only the quantity, as a variable in winter maintenance planning.

4.2. Why calcium and acetate deicers removed mass and NaCl did not

Within 30 wetting-drying cycles, NaCl behaved like water: both solutions filled pores and added mass, NaCl slightly less, probably because crystallizing salt reduced the pore volume available to the solution. Damage by NaCl is known to depend on concentration and on freezing, both of which were outside the scope of this test [2,13], so the result should not be read as evidence that NaCl is harmless to pavements.

The $CaCl_2$ result agrees with previous comparative studies that ranked $CaCl_2$ as the most damaging common deicer [15,16]. Two processes explain the accelerating loss. Chloride deicers leach calcium hydroxide from the paste [15], and drying concentrates the pore solution until calcium oxychloride can precipitate at room temperature [11,12]. Each drying stage therefore adds expansive product near the surface, and the loss grows as the surface weakens. The corrosion inhibitor slowed the process by a third over 30 cycles, but the rate between cycles 20 and 30 was still about 0.15% per cycle. Wang et al. likewise found that an inhibitor delayed the onset of damage without reducing the final damage [15]. We therefore see inhibited $CaCl_2$ as a way to extend the life of structures with embedded steel, not as a concrete-friendly deicer.

The potassium acetate result conflicts with Wang et al., who observed only minor scaling with this product [15]. Acetate anions complex calcium and raise portlandite solubility, which releases hydroxide and supplies potassium for alkali-silica reaction [14]; under wetting-drying, where fresh solution is repeatedly drawn into the surface, leaching can outpace carbonation. The difference may also reflect solution concentration, cycle regime or aggregate reactivity. Thermogravimetric analysis of the altered surface layer for portlandite content, and X-ray diffraction for oxychloride and Friedel's salt, would allow the two mechanisms to be separated. Until then, the data do not support the common assumption that acetate deicers are safe for concrete pavements.

4.3. Dense matrices are not immune

The silica-fume mortar had a water/binder ratio of 0.24 and a density of about 2310 kg/m ^{3}, properties associated with very low permeability [30]. Even so, immersion in 5% NaCl doubled its deformation over 300 h. If positive readings denote shortening, as the behavior of the sealed prisms suggests, the extra deformation of the immersed prisms points to two effects. External brine has a lower water activity than pure water, so it cannot relieve the self-desiccation of a low water/binder matrix as fully as water would, and chloride can accelerate hydration and the associated chemical shrinkage [23]. Friedel's salt formation and crystallization pressure, which reduce the flexural strength of cement paste in NaCl [13], add internal stress on top of this. Whichever mechanism dominates, a dense matrix is not a sufficient defense on its own; it slows the ingress of salt but does not prevent volume change once salt arrives.

4.4. Joints as the weak link

The survey shows that the most severe distress (blow-ups, spalls, joint offsets) is concentrated at joints, and the monitoring explains why. In a jointed pavement, thermal expansion is meant to be taken up by contraction joints, which close in summer, and by expansion joints, which absorb what the contraction joints cannot. Grit and deicing sand that enter contraction joints opened by winter contraction prevent them from closing again, and the pavement grows in length each season [20,21]. The joint movement at km 181 fits this picture. Assuming 5 m slabs, the total closure of 24.4 mm over about 150 m equals a mean strain of 163×10^{-6}, the free expansion for a mean slab temperature rise of about 16 °C, which is plausible between spring installation and June. The distribution was far from uniform: two joints took 29% of the closure, and 11 joints moved 0.5 mm or less. That pattern is what one expects when most joints are locked by incompressibles and the movement is forced into the few that still work.

Fig. 7b puts the expansion-joint spacing in context. With $\alpha = 10 \times 10^{-6}\,°C^{-1}$, a 15 mm expansion joint can absorb the free expansion of 50 m of pavement for a 30 °C rise in mean slab temperature, which is roughly the design case. At the 300-700 m spacing found in the Turkestan region, the same joint is used up by a rise of 2-5 °C, and a 40 °C seasonal rise would require 120-280 mm of movement. Once the expansion joints are full and the contraction joints are locked, the compressive force has nowhere to go but up, and blow-ups occur at the weakest joint, often one already weakened by scaling or spalling. This agrees with the absence of blow-ups in the cooler Zhambyl region and with their presence where surface temperatures of 59.5-70 °C were measured.

Deicers therefore act on joints in two ways. Chemically, they damage the joint faces, where solution collects and saturation is highest [20]; our $CaCl_2$ and acetate results show how quickly that can remove material. Mechanically, the sand and grit spread with them fill the joints, and the following summer turns that fill into compressive stress. Neither effect is addressed by current winter maintenance practice in the region.

4.5. Implications for practice in Kazakhstan

Four measures follow from the results. First, calcium-based deicers should be restricted on concrete pavements, and potassium acetate should not be assumed to be harmless until its effect on local concretes is confirmed by longer tests. Where $CaCl_2$ is used for its lower effective temperature, inhibited formulations delay damage but do not prevent it. Second, contraction joints should be cleaned and resealed each spring, before the pavement warms, so that sand and grit are removed before they lock the joints. Third, expansion joints on existing pavements should be restored to the designed spacing where blow-ups have occurred, and new pavements should keep the 50 m design spacing. Fourth, new concrete for these roads should meet frost-and-deicer exposure requirements, such as a water/cementitious-materials ratio not exceeding 0.40 and a specified air content, as in exposure class F3 of ACI 318-19 [31]; entrained air and supplementary cementitious materials remain the most reliable means of improving scaling resistance [32-35]. Cement type, pore structure and mechanical loading also influence resistance [36-38], and surface additions such as nano-silica show promise in pavement concrete [39].

4.6. Limitations

The study has five limitations. The thermal stresses are elastic estimates from assumed material properties and a single test. The deicer exposure used wetting-drying without freezing and a limited number of cycles, so it does not reproduce the combined freeze-thaw and salt exposure of the field; a scaling test to CEN/TS 12390-9 [28] is planned. Replicate statistics are not yet reported for the mass-change and deformation tests. The mortar tests cover one concentration and 300 h, and no microstructural analysis was performed. Finally, the joint monitoring covers one season at one site, and slab temperatures were not recorded during it. Continuous joint movement and slab temperature records through a full year would allow the trigger temperature for pavement growth to be estimated, as done for United States pavements by Chhay et al. [21].

5. Conclusions

Laboratory tests and a field survey of concrete highways in southern Kazakhstan lead to the following conclusions.

(1) Applying NaCl to an iced concrete surface at -5 °C cooled the surface to -14 °C within 1 min, a rate of about 14 °C/min. The surface-to-50 mm temperature difference of 8.9 °C corresponds to an elastic thermal stress of 2.7-3.3 MPa, close to the tensile strength of pavement concrete, which makes repeated thermal shock a plausible contributor to scaling.

(2) After 30 wetting-drying cycles, specimens in water and NaCl gained 2.2% and 1.5% mass, while those in $CaCl_2$, inhibited $CaCl_2$ and potassium acetate lost 5.2%, 3.5% and 5.0%. The loss under $CaCl_2$ accelerated with cycling.

(3) A nitrite-phosphate corrosion inhibitor reduced $CaCl_2$ mass loss by 33% at 30 cycles but did not stop it. Potassium acetate was nearly as damaging as $CaCl_2$, contrary to the view that acetates are harmless to concrete.

(4) A dense silica-fume mortar (water/binder ratio 0.24) immersed in 5% NaCl reached a length change of 0.66 mm/m in 300 h, 1.9 times that of sealed prisms, showing that low permeability alone does not prevent salt-related volume change.

(5) Expansion joints on the surveyed highways were 250-700 m apart instead of the designed 50 m, and contraction joints were packed with deicing grit. At 300-700 m spacing a 15 mm expansion joint is used up by a 2-5 °C rise in slab temperature, which explains the blow-ups recorded where pavement surfaces reached 59.5-70 °C.

(6) Thirty monitored joints closed by 0.81 ± 0.94 mm on average, and two joints took 29% of the total closure. Resealing joints each spring and restoring the design expansion-joint spacing should be priorities for the road operator, alongside restricting calcium-based and acetate deicers.

References

[1] HE Beck, NE Zimmermann, TR McVicar, N. Vergopolan, A. Berg, EF Wood, Present and future Köppen-Geiger climate classification maps at 1-km resolution, Sci. Data 5 (2018) 180214. https://doi.org/10.1038/sdata.2018.214

[2] GJ Verbeck, P. Klieger, Studies of "salt" scaling of concrete, Highw. Res. Board Bull. 150 (1957) 1-13.

[3] JJ Valenza II, GW Scherer, A review of salt scaling: I. Phenomenology, Cem. Concr. Res. 37 (2007) 1007-1021. https://doi.org/10.1016/j.cemconres.2007.03.005

[4] TC Powers, A working hypothesis for further studies of frost resistance of concrete, J. Am. Concr. Inst. Proc. 41 (1945) 245-272.

[5] MJ Setzer, Micro-ice-lens formation in porous solids, J. Colloid Interface Sci. 243 (2001) 193-201. https://doi.org/10.1006/jcis.2001.7828

[6] B. Lubelli, RPJ van Hees, HP Huinink, CJWP Groot, Irreversible dilation of NaCl contaminated lime-cement mortar due to crystallization cycles, Cem. Concr. Res. 36 (2006) 678-687. https://doi.org/10.1016/j.cemconres.2005.10.008

[7] JJ Valenza II, GW Scherer, Mechanism for salt scaling, J. Am. Ceram. Soc. 89 (2006) 1161-1179. https://doi.org/10.1111/j.1551-2916.2006.00913.x

[8] JJ Valenza II, GW Scherer, A review of salt scaling: II. Mechanisms, Cem. Concr. Res. 37 (2007) 1022-1034. https://doi.org/10.1016/j.cemconres.2007.03.003

[9] O. Çopuroğlu, E. Schlangen, Modeling of frost salt scaling, Cem. Concr. Res. 38 (2008) 27-39. https://doi.org/10.1016/j.cemconres.2007.09.003

[10] J. Zhang, J. Wang, Y. Li, J. Yuan, Y. Wu, Research progress on salt scaling and protective methods for concrete pavements, Constr. Build. Mater. 342 (2022) 127993. https://doi.org/10.1016/j.conbuildmat.2022.127993

[11] Y. Farnam, S. Dick, A. Wiese, J. Davis, D. Bentz, J. Weiss, The influence of calcium chloride deicing salt on phase changes and damage development in cementitious materials, Cem. Concr. Compos. 64 (2015) 1-15.

[12] P. Suraneni, VJ Azad, OB Isgor, WJ Weiss, Calcium oxychloride formation in pastes containing supplementary cementitious materials: thoughts on the role of cement and supplementary cementitious materials reactivity, RILEM Tech. Lett. 1 (2016) 24-30.

[13] C. Qiao, P. Suraneni, J. Weiss, Damage in cement pastes exposed to NaCl solutions, Constr. Build. Mater. 171 (2018) 120-127. https://doi.org/10.1016/j.conbuildmat.2018.03.123

[14] C. Giebson, K. Seyfarth, J. Stark, Influence of acetate and formate-based deicers on ASR in airfield concrete pavements, Cem. Concr. Res. 40 (2010) 537-545. https://doi.org/10.1016/j.cemconres.2009.09.009

[15] K. Wang, DE Nelsen, WA Nixon, Damaging effects of deicing chemicals on concrete materials, Cem. Concr. Compos. 28 (2006) 173-188. https://doi.org/10.1016/j.cemconcomp.2005.07.006

[16] D. Darwin, J. Browning, L. Gong, SR Hughes, Effects of deicers on concrete deterioration, ACI Mater. J. 105 (2008) 622-627.

[17] X. Shi, M. Akin, T. Pan, L. Fay, Y. Liu, Z. Yang, Deicer impacts on pavement materials: introduction and recent developments, Open Civ. Eng. J. 3 (2009) 16-27. https://doi.org/10.2174/1874149500903010016

[18] Z. Wu, C. Shi, P. Gao, D. Wang, Z. Cao, Effects of deicing salts on the scaling resistance of concrete, J. Mater. Civ. Eng. 27 (2015) 04014160. https://doi.org/10.1061/(ASCE)MT.1943-5533.0001106

[19] J. Jain, J. Olek, A. Janusz, D. Jóźwiak-Niedźwiedzka, Effects of deicing salt solutions on physical properties of pavement concretes, Transp. Res. Rec. 2290 (2012). https://doi.org/10.3141/2290-09

[20] W. Jones, Y. Farnam, P. Imbrock, J. Spiro, C. Villani, M. Golias, J. Olek, WJ Weiss, An overview of joint deterioration in concrete pavement: mechanisms, solution properties, and sealers, Joint Transportation Research Program, Purdue University, West Lafayette, IN, 2013.

[21] L. Chhay, YK Kim, SW Lee, Evaluation of trigger temperature for concrete pavement growth based on joint movement data, Constr. Build. Mater. 278 (2021) 121790. https://doi.org/10.1016/j.conbuildmat.2020.121790

[22] PK Mehta, PJM Monteiro, Concrete: Microstructure, Properties, and Materials, 4th ed., McGraw-Hill Education, New York, 2014.

[23] AM Neville, Properties of Concrete, 5th ed., Pearson Education, Harlow, 2011.

[24] GOST 12730.1-78, Concretes. Methods of determination of density, Interstate standard, Moscow, 1978.

[25] GOST 10180-2012, Concretes. Methods for strength determination using reference specimens, Interstate Council for Standardization, Metrology and Certification, Moscow, 2013.

[26] YH Huang, Pavement Analysis and Design, 2nd ed., Pearson Prentice Hall, Upper Saddle River, NJ, 2004.

[27] ASTM C672/C672M-12, Standard Test Method for Scaling Resistance of Concrete Surfaces Exposed to Deicing Chemicals (withdrawn 2021), ASTM International, West Conshohocken, PA, 2012.

[28] CEN/TS 12390-9:2016, Testing hardened concrete. Part 9: Freeze-thaw resistance with de-icing salts. Scaling, European Committee for Standardization, Brussels, 2016.

[29] PC Kreijger, The skin of concrete: composition and properties, Mater. Construction 17 (1984) 275-283.

[30] D. Wang, C. Shi, Z. Wu, J. Xiao, Z. Huang, Z. Fang, A review on ultra high performance concrete: Part II. Hydration, microstructure and properties, Constr. Build. Mater. 96 (2015) 368-377. https://doi.org/10.1016/j.conbuildmat.2015.08.095

[31] ACI Committee 318, Building Code Requirements for Structural Concrete (ACI 318-19) and Commentary, American Concrete Institute, Farmington Hills, MI, 2019.

[32] MT Hasholt, Air void structure and frost resistance: a challenge to Powers' spacing factor, Mater. Struct. 47 (2014) 911-923. https://doi.org/10.1617/s11527-013-0102-9

[33] Z. Liu, W. Hansen, Freezing characteristics of air-entrained concrete in the presence of deicing salt, Cem. Concr. Res. 74 (2015) 10-18.

[34] G. Skripkiūnas, D. Nagrockienė, G. Girskas, M. Vaičienė, E. Baranauskaitė, The cement type effect on freeze-thaw and deicing salt resistance of concrete, Procedia Eng. 57 (2013) 1045-1051. https://doi.org/10.1016/j.proeng.2013.04.132

[35] I. Afrani, C. Rogers, The effects of different cementing materials and curing on concrete scaling, Cem. Concr. Aggreg. 16 (1994) 132-139. https://doi.org/10.1520/CCA10291J

462 [36] J. Zhang, PC Taylor, Pore size distribution in cement pastes in relation to freeze-thaw stress, J.
463 Mater. Civ. Eng. 27 (2015) 04014123. https://doi.org/10.1061/(ASCE)MT.1943-5533.0001053
464 [37] W. Sun, YM Zhang, HD Yan, R. Mu, Damage and damage resistance of high strength concrete
465 under the action of load and freeze-thaw cycles, Cem. Concr. Res. 29 (1999) 1519-1523.
466 [38] J. Tian, W. Wang, Y. Du, Damage behavior of self-compacting concrete and prediction model
467 under coupling effect of salt freeze-thaw and flexural load, Constr. Build. Mater. 119 (2016)
468 241-250. https://doi.org/10.1016/j.conbuildmat.2016.05.073
469 [39] M. Gonzalez, SL Tighe, K. Hui, S. Rahman, A. de Oliveira Lima, Evaluation of freeze/thaw and
470 scaling response of nanoconcrete for Portland Cement Concrete (PCC) pavements, Constr.
471 Build. Mater. 120 (2016) 465-472.

Appendix A. Joint monitoring data, km 181, Almaty-Shelek-Khorgos highway

Table A.1. Joint and tell-tale widths (mm) at installation and at removal (June 2025).

Joint	Joint width, installed	Tell-tale width, installed	Joint width, removed	Tell-tale width, removed	Joint width change	Tell-tale width change
1	15.0	12.0	11.0	17.5	-4.0	+5.5
2	10.0	10.0	10.0	10.5	0.0	+0.5
3	12.0	12.0	11.0	12.4	-1.0	+0.4
4	9.0	9.0	9.5	11.0	+0.5	+2.0
5	9.0	9.0	8.5	9.5	-0.5	+0.5
6	11.0	11.0	9.0	11.2	-2.0	+0.2
7	8.0	8.0	7.5	9.1	-0.5	+1.1
8	8.0	8.0	8.0	9.5	0.0	+1.5
9	9.0	9.0	8.4	9.0	-0.6	0.0
10	11.0	8.0	8.0	9.8	-3.0	+1.8
11	8.0	8.0	7.9	8.5	-0.1	+0.5
12	8.0	9.0	8.9	10.5	+0.9	+1.5
13	10.0	10.0	9.8	10.0	-0.2	0.0
14	9.0	9.0	8.4	9.5	-0.6	+0.5
15	8.0	8.0	7.0	10.0	-1.0	+2.0
16	8.0	8.0	7.5	10.0	-0.5	+2.0
17	10.0	10.0	9.1	10.2	-0.9	+0.2
18	8.0	8.0	7.0	9.0	-1.0	+1.0
19	9.0	9.0	8.8	10.5	-0.2	+1.5
20	8.0	8.0	7.2	8.5	-0.8	+0.5
21	8.0	8.0	7.1	8.9	-0.9	+0.9
22	9.0	9.0	8.9	10.5	-0.1	+1.5
23	9.0	9.0	8.0	9.9	-1.0	+0.9
24	9.0	9.0	7.5	9.8	-1.5	+0.8
25	9.0	9.0	8.2	9.5	-0.8	+0.5
26	11.5	11.5	10.4	11.5	-1.1	0.0
27	9.0	9.0	7.9	9.5	-1.1	+0.5
28	10.0	10.0	8.8	10.0	-1.2	0.0
29	9.0	9.0	8.0	9.0	-1.0	0.0
30	8.0	8.0	7.8	10.0	-0.2	+2.0
Total					-24.4	+30.3

Joint 24: the original field sheet lists a change of -0.5 mm; the recorded widths (9.0 → 7.5 mm) give -1.5 mm, which is used here. Totals are recomputed from the recorded widths.